

MHD Dynamics and Error Fields in the RFX-mod2 Reversed field Pinch

P.Bettini, R.Cavazzana, G.Marchiori, L.Marrelli, G.Spizzo, D.Voltolina, P.Zanca

Consorzio RFX (CNR, ENEA, INFN, Università degli Studi di Padova, Acciaierie Venete SpA), Padova, Italy

Introduction: RFX-mod is a Reversed Field Pinch device ($R=2.0\text{m}$ / $a=0.459\text{m}$) that allowed performing experiments in regimes with a plasma current up to 2 MA [¹]. Due to its low value of the safety factor ($q<<1$) and the central peaking of current density, the RFP is characterized by the presence of MHD modes that, in RFX-mod, are controlled by a combination of a passive boundary and an active control system [²]. In order to reduce secondary MHD modes, a modification of the layout of the RFX-mod device is in progress [³] consisting in the removal of the Inconel vacuum vessel and a modification of the stainless steel supporting structure to be made vacuum tight. In the RFX-mod2 device the shell-plasma distance will decrease from $b/a=1.11$ to $b/a=1.04$ and copper, instead of Inconel, will be the conducting structure nearest to the plasma. MHD non-linear simulations predict a reduction of the amplitude of secondary tearing modes and consequently the edge bulging due to their phase locking is expected to decrease. Moreover, the plasma current threshold for tearing modes wall locking will significantly increase [⁴].

On the other hand, due to the reduced shell-plasma distance, the RFX-mod2 plasma will be even more sensitive to magnetic field errors at its boundary, produced by the shell eddy currents near the poloidal cut (also named gap) for the penetration of the electric and magnetic fields and the holes for diagnostic access. The amplitude of the error fields depends on the geometry of the gaps and on the time scale of the variations. Reference [⁵] considered the effect of plasma position control by external field shaping windings: given the relatively slow time scale, eddy currents are likely to be uniform along the radial direction of the passive structures (“thin-shell”). This study confirmed that the overlapped poloidal gap concept [²], developed for RFX-mod, represents a significant improvement in terms of error field passive reduction, compared to the original RFX butt-joint [⁶], and it has therefore been selected for RFX-mod2.

The aforementioned thin-shell approximation is not applicable to estimate error fields due to faster phenomena, related to MHD modes. In the Madison Symmetric Torus a regular sawtooth activity is observed: equilibrium current profiles slowly peak and suddenly flatten at the sawtooth crash, determining a fast inward displacement of the plasma column generating a large error field at the poloidal gap finally leading to wall locking of tearing modes [⁷]. Based on the similarity of the magnetic boundary with MST; it is expected that RFX-mod2 plasmas will experience a similar dynamics. The aim of this paper is to verify if the advantages of the overlapped concept will also apply to RFX-mod2 sawtooth crashes. A relative comparison of error fields between the butt joint and the overlapped shell design is performed in order to determine if wall locking of tearing modes can occur.

We use the code CAFE-hVI, which implements an integral formulation to solve for eddy currents on a polyhedral mesh of generic topology (i.e. including an arbitrary number of cuts and holes) with a very efficient topological pre-processing algorithm [⁸].

Model of a reconnection event. The determination of sawtooth eddy currents adopts a simplified vacuum approach: the plasma is modelled with a thin sheet of current flowing along a toroidal surface ($r=35\text{cm}$) inside the vessel. The poloidal dependence of the current on the surface is $\mathbf{J}(\vartheta, \varphi) = \nabla\phi(\vartheta, \varphi) \times \hat{\mathbf{n}}$ ($\hat{\mathbf{n}}$ is the unit vector normal to the toroidal surface), where the derivatives of the stream function ϕ for an $m=1, n=0$ harmonic are defined as $d\phi/d\vartheta = k$; $d\phi/d\varphi = \cos(\vartheta + \omega t)$. The constant k determines the amplitude of the

current and ω is the oscillation frequency for which the code computes the eddy currents in each volume element of the mesh.

Volumetric mesh geometries. The mesh is composed by hexahedra with parallel faces (parallelepipeds) whose vertices are located on concentric toroidal surfaces. The radial thickness of the copper shell (3mm) is split in 5 layers, in order to resolve the radial profile of the penetrated currents: the skin depth of copper at 10kHz is 0.6mm. Hexahedra vertices are equally spaced in the poloidal direction extending 6.5°, while their size in the toroidal direction ranges from 4.5° away from the edges down to 0.02° approaching the edges. Mesh elements are smaller in toroidal regions where strong gradients occur, as it is the case of the chosen internal source of vertical field simulating the plasma displacement. Such a non-uniform pattern is a compromise that allows obtaining an acceptable accuracy within reasonable computing times.

Eddy current patterns at high frequency. In toroidal regions away from the gap, eddy currents are essentially toroidal, independently of the shell gap design. Fig 1a) shows the poloidal dependence of the toroidal component for each layer of the mesh (green traces represent the imaginary part, indicating the delay in the penetration of current into the outer layers). The highest current occurs at the inner layer, which is nearer to the $m=1, n=0$ source (oscillating at 10 kHz in this case): the direction at the low field side is opposite compared to the high field side so that currents form a dipolar pattern. The toroidal current amplitude decreases in middle layers and it changes direction in outer layers. In lower frequencies regimes (< 1kHz) eddy currents in the layers are more similar, due to the much longer penetration depth, and patterns are almost identical to the ones obtained by the thin shell computations of the CAFE-BEM code⁹.

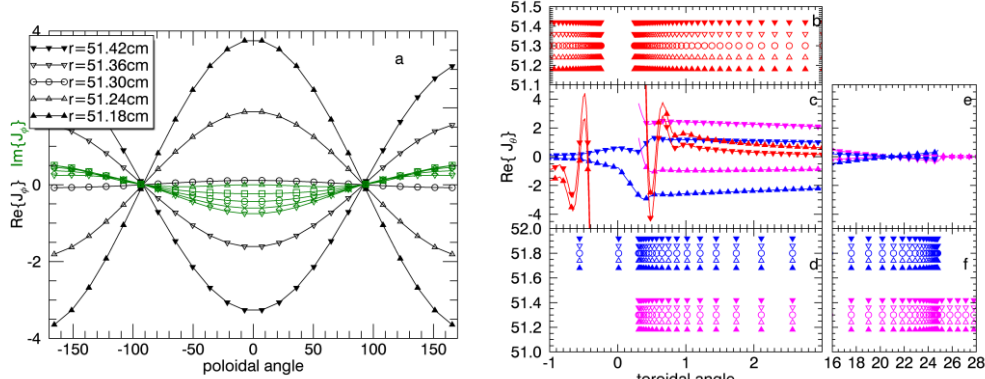


Fig. 1) a) Poloidal dependence of the real (black) and imaginary (green) part of the toroidal current for the five layers composing the conducting shell mesh ($\theta=0$ corresponds to the Low Field Side). b,d) radial position of barycentres of volume elements in a toroidal region around the shell poloidal edges for butt joint (red) and overlapped shell (blue upper sheet, magenta lower sheet). c,e) toroidal dependence of the real part of the poloidal currents at $\theta=90^\circ$ for the inner layers (upper triangles) and outer layers (lower triangles). Colors correspond to the different shell designs (as shown in b,d). The maximum value of poloidal currents for the butt joint case is 10 times higher than the y axis range.

Near the poloidal edges of the shell (both in the butt joint and in the overlap design), the dominant eddy current component is the poloidal one. Let us consider the butt joint design first: Fig.2b shows the radial and toroidal location of mesh volumes barycentre that gets denser towards the edges of the poloidal gap. The red curves in panel c) represent the toroidal dependence of the poloidal current: upper and lower triangles correspond to the inner and to the outer layer, respectively. The poloidal current appears concentrated on two facing and anti-symmetric narrow layers (becoming narrower as the frequency increases) and reaches very high values (± 40 in y axis units). The change of sign that takes place within half a degree

from the gap edges does not appear to be an artefact of the discretization, as the toroidal size of volume elements is much smaller than this feature. Moreover, the poloidal current profile does not change by further reducing the toroidal size of volumes.

As far as the overlapped gap design is concerned, panel d) shows the mesh volumes barycentre in the toroidal region around the edge of the inner sheet, while panel f) corresponds to the edge of the outer sheet. The maximum value of poloidal current is located at the inner edge (panel c, magenta curves represent the inner sheet, blue curves the outer sheet, upper and lower triangles indicate inner and outer layers, respectively) but it is 10 times lower than in the butt joint case. The currents at the outer edge (panel e) are significantly smaller. On the other hand, poloidal current is distributed all along the overlapped region and directions in inner and outer layers are opposite for each sheet. This striking difference of current patterns has profound consequences on the radial magnetic field at the plasma surface of RFX-mod ($r=0.495\text{m}$) and consequently on error fields.

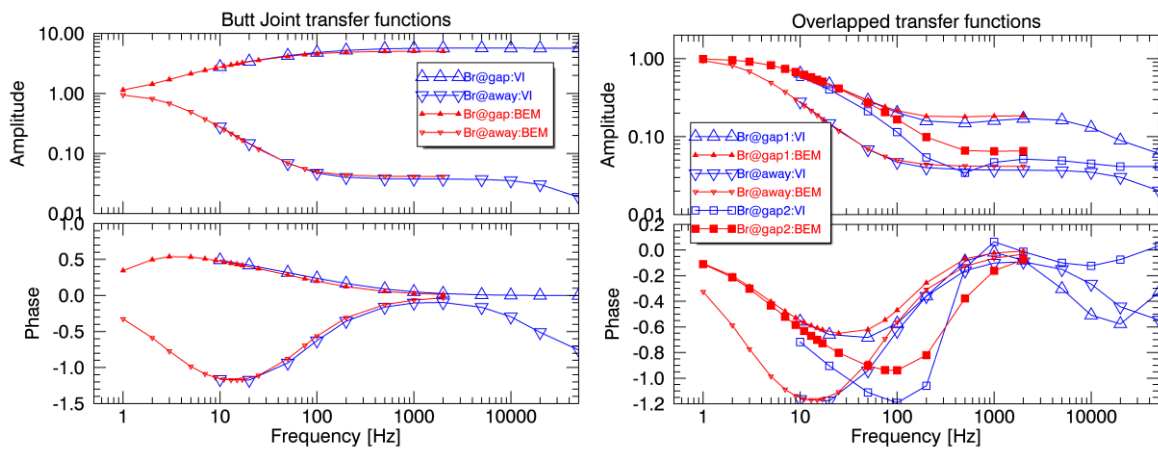


Fig.2) Amplitude (top panels) and phase (bottom panels) of the radial field at plasma radius, $\theta=90^\circ$ and toroidally near and away from shell edges. Left: Butt joint, Right: overlapped scheme. Red curves: thin shell CAFÉ_BEM; blue curves: volumetric meshes CAFÉ_hVI

Fig 2 shows the transfer functions (amplitude and phase) for the radial magnetic field near (upper triangles and squares) and far away (lower triangles) from the edges when the source is a toroidal surface with $m=1, n=0$ symmetry, as above. Red traces represents the radial field computed by means of the thin shell code (CAFÉ_BEM) while the blue ones are obtained through the volume integral code, CAFÉ_hVI. While for the butt joint case the two approaches yield similar results (at similar frequencies), a greater attenuation and phase delay occur for the radial field below the upper shell edge for the overlapped shell case (gap2: square symbols).

Error fields due to a reconnection event. The generic time evolution of the radial field at a given location is determined by Fourier decomposing the current source time trace, multiplying by the transfer functions and finally performing an inverse Fourier transform. As a first rough estimate, we consider an inward displacement of 0.5cm: Shafranov B_{vadd} formula [5] gives an additional vertical field of 1mT. We therefore determine the current source time behaviour so that the $m=1, n=0$ harmonic of b_r at plasma radius increases in $250\mu\text{s}$ and then remains constant (thick black trace in Fig.3a). Fig 3b and c display the time evolution of the radial field at $r=0.495$ and $\theta=90^\circ$ in a toroidal region around the shell edges (at $\phi=0^\circ$ for the butt joint, and 5° and 24° in the overlapped shell). A significant localized radial field enhancement takes place for the butt joint: a very high radial field (up to 150mT) is concentrated in toroidal region extending few degrees. Though qualitatively similar to the error field shape during the start-up phase [4], it affects a narrower toroidal region. Red

dashed and dotted time traces in panel a represent the time behaviour of the field for two angles as depicted in panel c. A significant reduction (by a factor 10-20) of error field occurs in the overlapped concept (panel b). Interestingly, in the latter case, the error field evolves in two phases: initially (between 0.1 and 0.75ms), only one peak occurs, located at the inner edge of the copper shell; later on, a second lower peak, corresponding to the outer edge of the overlapped shell appear. The error field pattern of this later phase is also qualitatively similar to the start-up error described in [4].

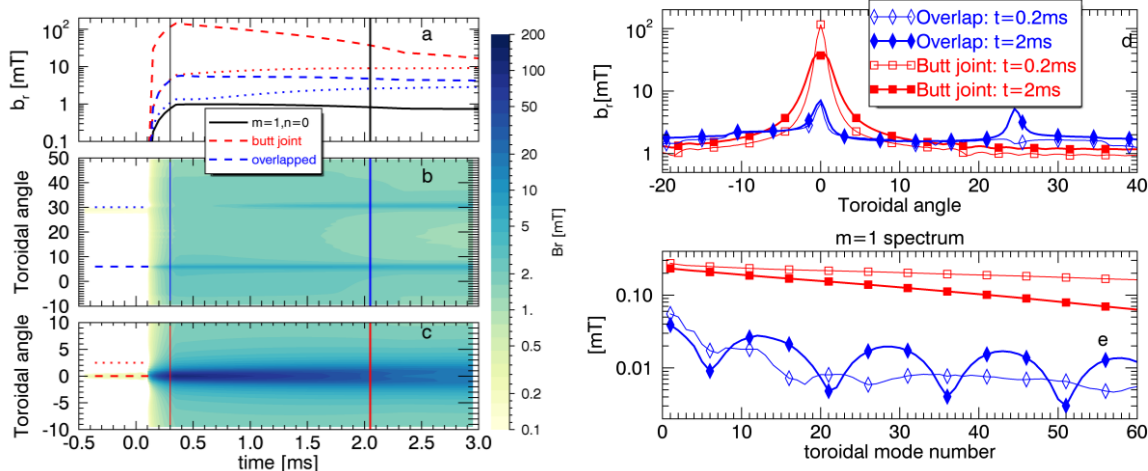


Fig.3) Time evolution of radial error field during a reconnection event for overlapped (b) and butt joint (c) design. Panel a show time traces in selected locations and the $m=1, n=0$ harmonic. d): error field profiles at $t=0.2\text{ms}$ and at 2ms ; e): corresponding $m=1$ spectra.

The shape of the error field has important consequences on the the $m=1$ spectrum which influences the dynamics of resonant MHD modes. As shown in Fig. 3e) the butt-joint $m=1$ harmonic spectrum is almost flat, having significant amplitude in the resonant interval $n>6$. As time proceeds, the radial field peak broadens and therefore the higher n harmonics in the Fourier spectrum decrease. As far as the overlapped geometry is concerned, the Fourier spectrum in the first 0.5ms is similar to the butt-joint case (i.e. monotonically decreasing), but significantly attenuated. Later on, 1ms after the crash, it displays the characteristic interference pattern shown in reference [4] for a simulation of the RFX-mod2 start-up phase.

Summary: At high frequency, i.e. on faster time scales, the difference between the overlapped and the butt joint scheme is even more dramatic than in the start-up case (modelled in [4] by an increase of a 30mT external vertical field in 20ms, i.e. the typical raise time of the RFP plasma current). Even though the error field is highly localized in the first phase, its amplitude is significantly reduced: this confirms that the overlapped gap design, which is under implementation in RFX-mod2, is considerably better for an RFP boundary.

¹ Martin P., Nucl. Fusion 51 (2011) 094023

² Sonato P. et al., Fus. Eng. Des. (2003) 161 66–8

³ Peruzzo S. et al., Fus. Eng. Des. (2019) (<https://doi.org/10.1016/j.fusengdes.2019.01.057>)

⁴ Marrelli L. et al., Nucl. Fusion 59(2019) 076027

⁵ Marrelli L. et al., Fus. Eng. Des. (2019) (<https://doi.org/10.1016/j.fusengdes.2019.01.054>)

⁶ Rostagni G., Fusion Eng. Des. 25 (1995) 301

⁷ Almagri, A.F. et al., Phys. Fluids B 4 (1992) 4080

⁸ Bettini P., et al., IEEE Trans. Mag. 53 (2017) 7204904

⁹ Bettini P. et al. IEEE Trans. Mag. (2014) 50 7000904